A new instrument for the IRTF: the MIT Optical Rapid Imaging System (MORIS)

A.A.S. Gulbis[1,2], J.L. Elliot[2], F. E. Rojas[2], S.J. Bus[3], J.T. Rayner[3], W.E. Stahlberger[3], A.T. Tokunaga[3], E.R. Adams[2], M.J. Person[2]

[1]Southern African Large Telescope (SALT) and South African Astronomical Observatory (SAAO), [2]Massachusetts Institute of Technology (MIT), [3]Univ. of Hawaii Institute for Astronomy (IfA)

NASA's 3-m Infrared Telescope Facility (IRTF) on Mauna Kea, HI plays a leading role in obtaining planetary science observations. However, there has been no capability for high-speed, visible imaging from this telescope. Here we present a new IRTF instrument, MORIS, the MIT Optical Rapid Imaging System. MORIS is based on POETS (Portable Occultation Eclipse and Transit Systems; Souza et al., 2006, PASP, 118, 1550). Its primary component is an Andor iXon camera, a 512x512 array of 16-micron pixels with high quantum efficiency, low read noise, low dark current, and full-frame readout rates of between 3.5 Hz (6 e~/pixel read noise) and 35 Hz (49 e~/pixel read noise at electron-multiplying gain=1). User-selectable binning and subframing can increase the cadence to a few hundred Hz. An electron-multiplying mode can be employed for photon counting, effectively reducing the read noise to sub-electron levels at the expense of dynamic range. Data cubes, or individual frames, can be triggered to nanosecond accuracy using a GPS. MORIS is mounted on the side-facing widow of SpeX (Rayner et al. 2003, PASP, 115, 362), allowing simultaneous near-infrared and visible observations. The mounting box contains 3:1 reducing optics to produce a 60 arcsec x 60 arcsec field of view at f/12.7. It hosts a ten-slot filter wheel, with Sloan g', r', i', and z', VR, Johnson V, and long-pass red filters.

We describe the instrument design, components, and measured characteristics. We report results from the first science observations, a 24 June 2008 stellar occultation by Pluto. We also discuss a recent overhaul of the optical path, performed in order to eliminate scattered light.

This work is supported in part by NASA Planetary Major Equipment grant NNX07AK95G.We are indebted to the University of Hawai'i IfA machine shop, in particular Randy Chung, for fabricating instrument components.

hardware:

- Andor iXon^{EM+} camera
- small-form, Windows-based computer
- GPS
- lenses and mirror for 3:1 focal reduction
- 10-slot filter wheel
- light-tight foreoptics box to mount camera to SpeX and enclose optics

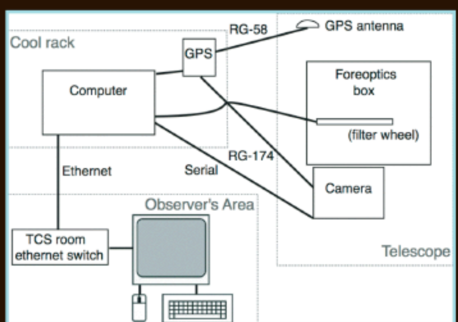

Fig. 2. Schematic drawing of the MORIS setup.The "cool rack" refers to one of four thermally-isolated cabinets around the perimeter of the IRTF Multiple Instrument Mount. The IRTF ethernet allows remote access to the instrument computer via the standard IRTF VNC interface.

Components

Andor iXon^{EM+} DU-897 camera:
E2V CCD97
thermoelecric cooling
trigger from GPS (sequence or each frame)
muliple readout modes (see characteristics)

Computer :
Shuttle XPC SD30G2
dual-core, 3.2GHz processor
2GB RAM; 10,000 rpm, dual hard drives

GPS:
Spectrum Instruments Intelligent Reference TM-4
programable output pulses as well as pps
< 1μsec timing accuracy

Light-tight foreoptics box :
filter wheel:
custom-built wheel with ten, 1" diameter slots
rotated by an Animatics Smartmotor
filters made by Asahi Spectra Inc.
fold mirror:
protected silver coating (>90% reflectivity)
lenses:
custom-made by Kreischer Optics, Ltd.
Schott SF5 or BK7
antireflective MgF_2 coating (<3.5% reflectance)

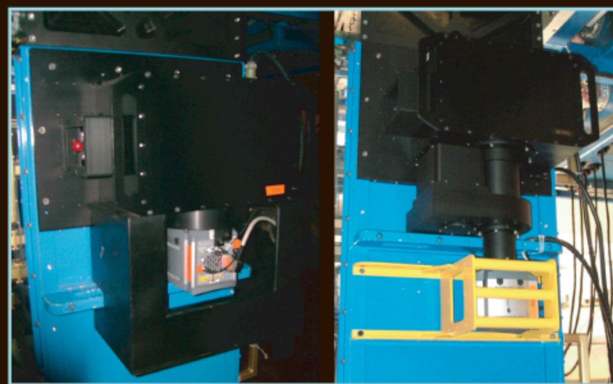

Fig. 1. MORIS mounted on SpeX. *(left)* Original configuration, 05/2008-05/2010. *(right)* Revised configuration, 08/2010. The black, anodized components are the light-tight foreoptics box.The grey camera is surrounded by a black (*left*) or yellow (*right*) protective cage. The computer and GPS are housed in an IRTF cool rack.

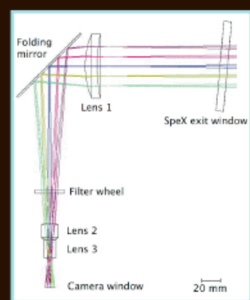

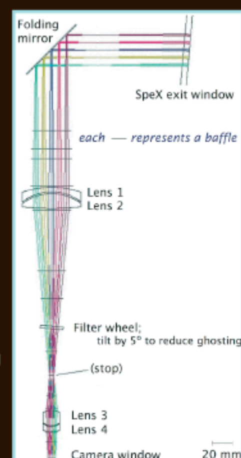

Fig. 3. ZEMAX diagrams of the MORIS optical path. *(left)* Original configuration, 05/2008 - 05/2010. (*right*) Revised configuration, 08/2010.The critical design changes were to include a stop and to introduce a series of baffles. A fold mirror is required to allow clearance for other instruments in the IRTF's Multiple Instrument Mount. All components shown in these diagrams are housed in the light-tight foreoptics box.

characteristics:

- high sensitivity, with QE > 90% across visible range
- low read noise and dark current
- high speed,capable of a few to hundreds of full frames per second
- selection of four amplifiers, each with three gains
- electron-multiplying capability
- can use a dichroic to take simultaneous NIR data with SpeX

Beam speed	f/12.7
Field of view	60 arcsec × 60 arcsec
CCD	E2V CCD97; 512 × 512, 16μm² pixels
Plate scale	0.117 arcsec/pixel
Readout rate	3.5 frames/sec (full frame, 1MHz amplifier);
	35 frames/sec (full frame, 10 MHz amplifier);
	to hundreds of frames/sec with binning and/ or subframing
Read noise	5.83, 6.35, 8.58 e⁻ (1 MHz conventional; 5x, 2.4x, 1x gain)
	9.49, 10.04, 13.56 e⁻ (3 MHz conventional; 5x, 2.4x, 1x gain)
	0.30, 0.36, 0.56 e⁻ (1 MHz EM[a]=40; 5x, 2.4x, 1x gain)
	0.40, 0.47, 0.78 e⁻ (3 MHz EM[a]=40; 5x, 2.4x, 1x gain)
	0.08, 0.26, 0.42 e⁻ (5 MHz EM[a]=100; 5x, 2.4x, 1x gain)
	0.18, 0.28, 0.45 e⁻ (10 MHz EM[a]=100; 5x, 2.4x, 1x gain)
Gain	0.66, 1.47, 3.70 e⁻/ADU (1 MHz conventional; 5x, 2.4x, 1x gain)
	1.78, 3.89, 9.78 e⁻/ADU (3 MHz conventional; 5x, 2.4x, 1x gain)
	0.06, 0.12, 0.29 e⁻/ADU (1 MHz EM[a]=40; 5x, 2.4x, 1x gain)
	0.13, 0.28, 0.69 e⁻/ADU (3 MHz EM[a]=40; 5x, 2.4x, 1x gain)
	0.05, 0.12, 0.28 e⁻/ADU (5 MHz EM[a]=100; 5x, 2.4x, 1x gain)
	0.05, 0.12, 0.30 e⁻/ADU (10 MHz EM[a]=100; 5x, 2.4x, 1x gain)
Dead time	1.7 msec (for 512 rows at the default vertical shift speed)
Dark current[b]	< 0.001 e⁻/pix/sec
GPS timing accuracy	< 1 μsec[c]
GPS antenna cable delay	77 nsec[d]
GPS trigger cable delay	30.8 nsec[d]
Current filters	SDSS *g'*, *r'*, *i'*, and *z'*; Johnson *V*; *VR*; OG590 (long-pass red)

[a]Electron multiplying mode. Strength is chosen to illustrate sub-electron read noise.
[b]Dark current is negligible in exposures up to 240s at -70° C. This value represents the manufacturer's specification.
[c]Manufacturer's specification is ±25 nsec from UTC, with root-mean-square stability of 12.5 nsec.
[d]Based on manufacturer's specified time delay of 1.54 nsec/ft, for 50 ft. of RG-58 and 20 ft. of RG-174 coaxial cable.

SpeX 0.95-micron dichroic — SpeX 0.8-micron dichroic

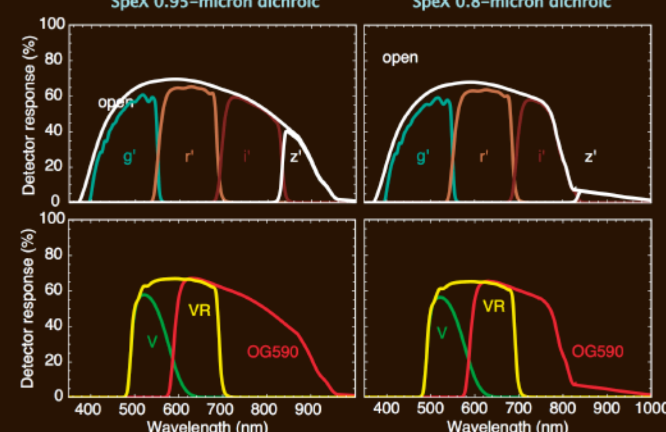

Fig. 4. The MORIS detector response as a function of wavelength. The response is shown as a percentage of light entering the telescope and thus includes throughput from all optics as well as CCD quantum efficiency. The two columns correspond to the SpeX 0.95-μm and 0.8-μm dichroic beam splitters,one of which must be selected to direct light out of the side-facing exit window and into the MORIS foreoptics box. Responses are shown for (*top*) open (no filter) and the Sloan filters and (*bottom*) the other supported filters.All filters were made by Asahi Spectra.

first science:

stellar occultation by Pluto (24 June 2008)

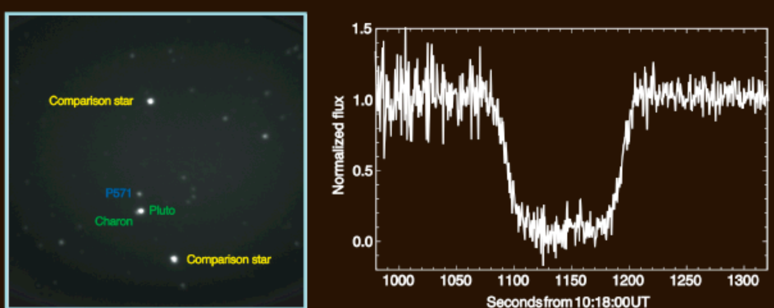

Fig. 5. *(left)* Raw MORIS image of the Pluto field. This is a 5-second exposure, binned 2x2, taken an hour before the occultation. The SpeX 0.95-μm dichroic was in place are there was no filter. Pluto, its moon Charon, the occultation star (P571 by McDonald & Elliot, AJ, 120, 1599, 2000; *R*=15.8 USNOB),and the comparison stars used to generate the light curve are all apparent. The image has been scaled to display analog-to-digital units (ADUs) 0 to 20,000 in order to highlight fainter features. The two comparison star peak counts are on the order of 50,000 ADU/pixel, and Pluto's peak counts are approximately 40,000 ADU/pixel. A slight vignetting by one of the optical holders is apparent at the corners of the frame. In addition, there is a gradient in the background light that decreases radially by a factor of approximately 1.5 from the center to the edges.This gradient was due to scattered light, which has been eliminated in the revised design (see Fig. 7). *(right)* Light curve from the occultation of P571 by Pluto.The noise in the baseline prior to immersion is the result of scattered clouds throughout the observation.The data were taken in 1 MHz conventional 2.4x mode, at a rate of 4 Hz. Raw data frames were used to generate this lightcurve, with a circular aperture of 12 superpixels diameter and normalization by the mean of the two comparison stars. This light curve is binned by two in time to return a SNR of 56 per atmospheric scale height of 60 km on Pluto. Using 5-second frames taken 0.75-1 hour before and 1 - 1.25 hours after the occultation, we determined a background ratio for (Pluto + Charon) / (Pluto + Charon+P571) of 0.826 ± 0.001.

extrasolar planetary transit by XO-2b

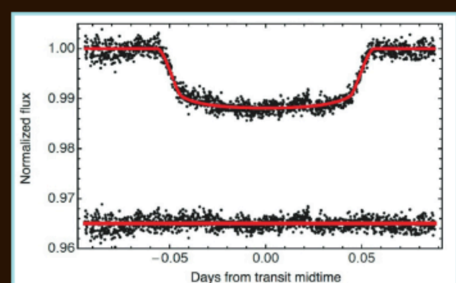

Fig. 6. MORIS light curve from a transit of exoplanet XO-2b. Exposures were 2 seconds, using the SpeX 0.95-micron dichrioc and a Thor Labs long-pass-red filter (cutting on at 700 nm). The data were taken in full frame, 1 MHz conventional 2.4x mode. (*top*) Normalized flux of the star is plotted versus time, usng a 30-pixel radius aperture. Black dots represent data binned by ten seconds and the red line is the model fit. The transit light curve was fit using the Mandel & Agol (ApJ, 580, L171, 2002) algorithm as implemented by the white-noise model described in Carter & Winn (ApJ, 704, 51, 2009). We assumed that XO-2b has zero obliquity, oblateness, and orbital eccentricity and employed a quadratic limb-darkening law assuming T=5340 K, log *g*=4.48, [M/H]=0.5, and V_{micro}=2 km/s. We used the initial values of u_1= 0.3670 and u_2=0.2850 from Claret (A&A, 428,1001, 2004) and fit for the linear term, u_1, while leaving u_2 fixed. The best model parameters were found using a Monte Carlo Markov chains (MCMC) method, with the best least-squares-fit values used as initial parameters. Three independent chains of 106 links (minus the first 50,000 points in each) were combined to derive the final parameters, which are the median and 68.3% credible interval values (see Adams AJ, 714, 13, 2010). The orbital period was fixed to P = 2.615864 days, and we assumed that M*=0.971± 0.034 M_{sun}, R*=0.976± 0.024 R_{sun}, and M_{planet} = 0.565± 0.054 $M_{Jupiter}$ (Fernandez et al. AJ, 137, 4911, 2009). (*bottom*) The residuals between the data and the model are plotted versus time, with a red line at 0.

Results:

- decent-quality occultation data on a night of scattered clouds
- SNR of 56 per atmospheric scale height on a 15.8 mag star
- best-fit midtime 10:37:04.06 ± 00:00:00.54 and distance from shadow center 471± 12 km
  [assuming Elliot et al. 2007 (AJ, 134,1) atmospheric parameters]

- planetary radius R_{planet} = 0.955 ± 0.024 $R_{Jupiter}$
- midtime, 2454806.94750 ± 0.00027 BJD_{TDB}
- no signs of transit timing variation
- photometric precision of 0.5 mmag in 2 min.; midtime timing precision of 23 sec.

post-revision

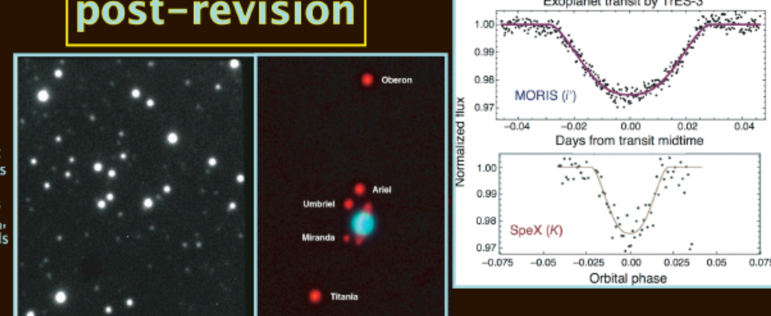

Fig. 7. August 2010 data from MORIS with the revised optical path. (*left*)Berkeley 81 open cluster, 120-sec. exposure in *V*. There is no evidence of scattered light (background varies < a few %) and stars are circular across the field. (*middle*) MORIS + SpeX data of Uranus in *g'* (blue), CH_4 (green), and *K* (red). (*right*) Data from an exoplanet transit by TrES-3 reaching accuracy of 1 mmag (MORIS) and 5.5 mmag (SpeX) in 2 min.